

# SOLUBILITIES OF BLOWING AGENT BLENDS

*G. Li, S. N. Leung, J. Wang, C.B. Park*

*Microcellular Plastics Manufacturing Laboratory*

*Department of Mechanical & Industrial Engineering, University of Toronto*

## **Abstract**

The solubility of HFC 134a and HFC 152a in polystyrene melt was measured up to 800 psi at 150 °C and 190 °C. A magnetic suspension balance was used to experimentally measure the apparent solubility. The Simha-Somcynsky (SS) equation of state (EOS) was applied in the multi-components system to estimate the swollen volume. Consequently, the buoyancy compensation can be obtained to determine the solubility of the blowing agent blends in the polymer melt.

## **Introduction**

Polymeric foams with desired cellular structures have resulted in advanced technological applications due to their improved mechanical, thermal, and acoustical properties [1, 2]. A variety of physical blowing agents (PBAs) are currently used in the plastic foam industry. Long-chain, physical blowing agents such as chlorofluorocarbon (CFCs), Hydrochloro- fluorocarbons (HCFCs), Hydrofluorocarbons (HFC), butane, or pentane have been used for low-density foam processing because of their low diffusivity and high solubility [3]. CFCs, however, are environmentally hazardous substances. The depletion of the stratospheric ozone layer associated to their uses has led to the introduction of the Montreal Protocol in 1987. According to the Protocol, the production of CFCs has been banned in Europe and United States since 1995. As the alternatives to CFCs, HCFCs provided the opportunity to expedite the phaseout of CFCs without disrupting the societal benefits derived from CFC products. However, because of the ozone-depleting potential of HCFCs as transitional substances, the protocol indicates that the basic phase-out schedule for HCFCs in developed countries is as follows based on the terms of the Montreal Protocol: 35% reduction in 2004, 65% reduction in 2010, 90% reduction in 2015, 99.5% reduction in 2020, and complete phaseout in 2030. Furthermore, according to U.S. Environmental Protection Agency's (EPA's) Significant New Alternatives Policy (SNAP) program which implements Section 612 of the Clean Air Act Amendments of 1990, the most commonly used HCFCs for foam blowing agents (i.e. HCFC-141b, HCFC-22 and HCFC-142b) will be phased out at an even earlier time. HCFC-141b was prohibited in the U.S. on January 1, 2003. The import of HCFC-141b is forbidden. The production of HCFC-141b is allowed in the U.S. only if it is going to be exported to other countries. HCFC-22 and HCFC-142b will be phased out on January 1, 2010.

Therefore, it is an urgent issue to find the next generation of environmentally benign substances which can be used as a replacement for CFCs and HCFCs in foam manufacturing. Currently, extensive research has been devoted to develop new blowing agents for foam production [4-8]. The potential blowing agent replacement candidates will be HFCs (134a, 152a, or experimental HFCs), hydrocarbons (HCs) and inert gases such as carbon dioxide (CO<sub>2</sub>) and nitrogen (N<sub>2</sub>). Among these conceivable surrogated gases, HFCs, i.e., HFC 134a and HFC 152a, offer superior thermal insulation capabilities and are desirable candidates for the replacement of CFCs and HCFCs [9-11]. Nevertheless, the low solubility and low diffusivity associated with HFC 134a [10, 12] has made the foaming processes

challenging despite its reasonably good R-value. In order to obtain low-density foams, it is necessary to employ high system pressure to increase the dissolved HFC 134a content. Previous research has demonstrated that the use of high HFC 134a content would lead to foams exhibiting a rather poor morphology. Gendron *et al.* [10] indicated that foaming polystyrene (PS) with HFC-134a content above 7.5 wt.% would result in large voids, which were in the order of a few millimeters, due to the inhomogeneous dissolution of the HFC 134a. On the other hand, it is known that HFC 152a has a higher solubility and diffusivity. However, there are serious concerns regarding the storage and long term insulation performance of the end-product due to its flammability and fast diffusion coefficient at room temperature. Moreover, it is believed that the rapid diffusion of HFC 152a will significantly decrease the amount of gas that will remain in the foam over time and deteriorate the thermal insulation efficiency of the product over its lifetime (ageing). In order to circumvent the aforementioned problems, blending the primary PBA with a secondary co-blowing agent can serve as a new processing path to control the foam quality. The main PBA is chosen for its expansion performance while the co-blowing agent is selected to stabilize the foaming processes [10]. Although it is a common industrial practice to utilize mixture of gases in polymeric foaming processes, scientific information of the role of each PBA component during the foaming process is very scarce in current literature. Furthermore, for optimal process design, the solubility data of gases mixtures in polymers is essential.

Solubility of various gases in polymer melts has been investigated by several authors. Sato *et al.* [13-17] studied the dissolution of carbon dioxide (CO<sub>2</sub>) and nitrogen (N<sub>2</sub>) in polystyrene (PS), polypropylene (PP), high-density polyethylene (HDPE), and poly(vinyl acetate) (PVAc) at 313 – 473 K and pressures up to 20 MPa. Areerat *et al.* [18] investigated the solubility of supercritical carbon dioxide (sc-CO<sub>2</sub>) in LDPE, HDPE, and PP. Li *et al.* [19, 20] studied the solubility of CO<sub>2</sub> in polypropylene (PP) and polylactide (PLA). However, these experimental measurements were restricted to a single-gas/single-polymer system.

In this paper, a methodology to measure the solubility of gases mixture in a polymer melt was developed. Similar to the single-gas/single-polymer system, the experimentally-measured apparent solubility data were corrected with respect to the swollen volume of the polymer/gases mixture. Although precise experimental data of pressure-volume-temperature (PVT) relationship of a polymer/gases mixture would be ideal for determining the swollen volume, technical difficulties associated with the experimental measurement of the data under high pressure and high temperature conditions have limited the availability of the data. Therefore, the Simha-Somcynsky (SS) EOS [21-24] was employed in this work to estimate the PVT information of the multi-component system.

## Experimental

### Materials

The plastic material used in this study is Polystyrene (PS, Styron PS685D) from The Dow Chemical Company with a melt flow index of 1.5 g/10 mi. Its specific gravity and glass transition temperature are 1.04 g/cm<sup>3</sup> and is 108 °C, respectively. The blowing agent blends used in this study are HFC-134a (SUVA<sup>®</sup> 134a), HFC-152a (Formacel<sup>®</sup> Z-2) and HFC 134a/152a blend (50:50 weight ratio) provided by Dupont.

### Apparatus and experimental procedures

The magnetic suspension balance (MSB) [25] from Rubotherm GmbH, was employed to measure the solubility of HFC-134a/HFC-152a blends in PS. A schematic diagram of MSB and the working procedures are shown in Fig. 1.

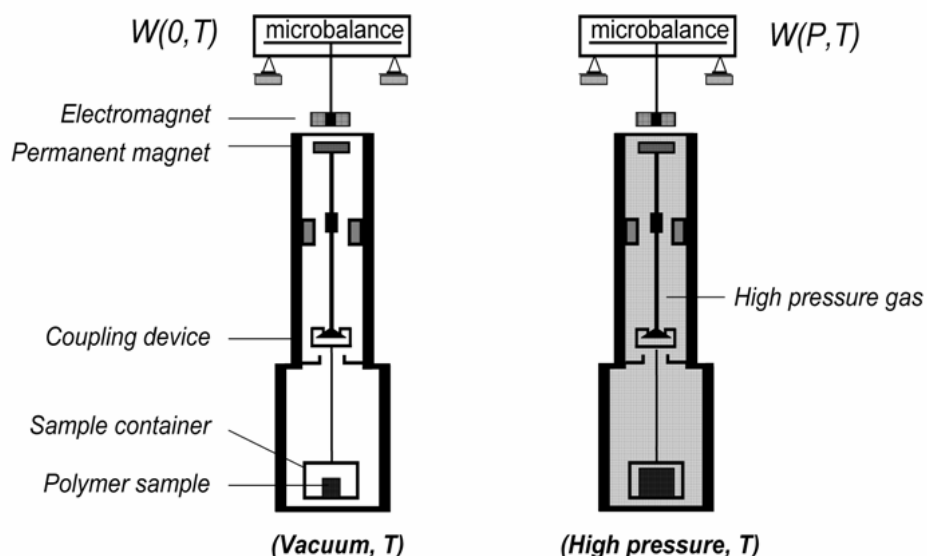


Figure 1 Schematic of Magnetic Suspension Balance (MSB)

The solubility data can be obtained by the following procedures:

- STEP 1. A 3 mm thick disk of polymer sample (approximately 0.5 gram) is precisely weighted and placed in the sample container in the absorption chamber.
- STEP 2. The absorption chamber is sealed and preheated to a designated temperature by a Julabo TD-6 Heating Circulator, which will also be used to precisely control the temperature of the chamber throughout the measuring process.
- STEP 3. The sample is degassed in vacuum until the mass becomes stable. The reading of the balance at vacuum (i.e.,  $P \approx 0$ ) and temperature ( $T$ ) was recorded as  $W(0, T)$ .
- STEP 4. High pressure gas is introduced into the sorption chamber and maintained at the desired pressure by a syringe pump (260D, ISCO). The high pressure gas starts to permeate into the polymer sample.
- STEP 5. Once the sample is saturated with gas (i.e., the mass of the polymer sample becomes stable), the reading of the balance is recorded as  $W(P, T)$ , where  $P$  is the saturation pressure and  $T$  is the system temperature.
- STEP 6. Finally, the amount of gas dissolved in the polymer,  $W_g$ , can be calculated by using the following equation:

$$W_g = W(P, T) - W(0, T) + \rho_{gas} (V_B + V_P + V_S) \quad (1)$$

where  $\rho_{gas}$  is the density of gas, which can be measured in-situ by the MSB [26];  $V_B$ ,  $V_P$ , and  $V_S$  are the volume of the sample holder (i.e., the sample container and the measuring load coupling device), the pure polymer sample, and the polymer swollen volume, respectively.  $V_P(P, T)$  can be determined using the Tait's equation of polystyrene:

$$V_P = \left[ 0.9742 + 0.0005996(T - 376.37) \right] \times \left[ 1 - 0.0894 \ln \left( 1 + \frac{P}{179.784 \exp(-0.004761T - 376.37)} \right) \right] \quad (2)$$

By ignoring the polymer's swollen volume ( $V_S$ ), the measured weight gain can be treated as the apparent solubility (Eq. 3),  $X_{apparent}$ , which is less than the actual solubility.

$$X_{apparent} = \frac{W(P, T) - W(0, T) + \rho_{gas} (V_B + V_P)}{\text{mass of sample}} \quad (3)$$

## Theoretical Framework

### Correction for the swollen volume contributed buoyancy effect

As shown in Eq. 1, it is important to know the swollen volume ( $V_S$ ) in order to accurately measure the solubility of the gas in the polymer melt. The buoyancy effect correction on the apparent solubility data is critical, especially under the circumstance of a high gas density and a large amount of swollen volume. However, the swollen volume of a polymer-gas mixture is difficult to measure physically. As a result,  $V_S$  is usually obtained from the total mass change of the polymer sample and the specific volume of the polymer-gas mixture ( $V_{sp,mix}$ ), which is calculated using an EOS. In this study, the SS-EOS (i.e., Eqs. 4 and 5) is an adopted calculation of the  $V_{sp,mix}$  of the polymer-gas mixture.

$$\tilde{p}\tilde{V}/\tilde{T} = (1-\eta)^{-1} + \frac{2yQ^2(1.011Q^2 - 1.2045)}{\tilde{T}} \quad (4)$$

$$\left( \frac{s}{3c} \right) \left[ \frac{s-1}{s} + \frac{\ln(1-y)}{y} \right] = \frac{\eta-1/3}{1-\eta} + \frac{y}{6\tilde{T}} Q^2 (2.409 - 3.033Q^2) \quad (5)$$

Consequently, the corrected solubility,  $X_{corrected}$ , with the buoyancy effect compensation can be obtained using Eq. 6.

$$X_{corrected} = X_{apparent} + \frac{\rho_{gas} \times V_S}{\text{mass of sample}} \quad (6)$$

### Determination of the theoretical solubility of gas in polymer melt

In a system containing several phases, the phase equilibrium among these phases should meet certain thermodynamic requirements. It is obvious that all the phases should attain the same temperature (T) and pressure (P) under equilibrium. Therefore, according to the classical thermodynamics [27, 28]

when the system is in phase equilibrium at constant T and P, the chemical potential,  $\mu_i$ , of component  $i$  in different phases (e.g.,  $\alpha, \beta, \dots$ ) must be equal as indicated in Eq. 7.

$$\mu_i^\alpha = \mu_i^\beta = \dots \quad (7)$$

Eq. 7 is the general condition for the phase equilibrium in a closed system and the thermodynamic basis for formulating problems in such a system. It also serves as the basis to calculate the theoretical solubility of gases in a polymer melt.

### 1. Pure gas dissolved in a polymer melt (binary mixture system)

When pure single gas was investigated, the equilibrium was between the vapor phase and the polymer-gas mixture phase. Due to the macromolecular structure, it was assumed that the polymer does not dissolve into the vapor phase; therefore, only the gas component would exist in the vapor phase. According to the phase equilibrium theory (i.e., Eq. 7), the mass fraction of the gas dissolved in the polymer melt, i.e. the theoretical solubility  $X_{theory}$ , can be calculated from solving Eq. 8 in equilibrium.

$$\mu_i^G(P, T) = \mu_i^P(P, T, X_{theory}) \quad (8)$$

where  $\mu_i^G$  is the chemical potential of the gas in the vapor phase and  $\mu_i^P$  is the chemical potential of the gas in the polymer-gas solution phase.

According to SS-EOS, Eq. 9 was used to calculate the  $\mu_1^G$  [21, 22, 23, 29, 30],

$$\begin{aligned} \frac{\mu_1^G}{RT} = \frac{G}{RT} = \ln y + s \frac{1-y}{y} \ln(1-y) - c[\ln(v^*(1-\eta)^3 / Q)] \\ - \frac{3}{2} c \ln \frac{2\pi m RT}{(N_a h)^2} + \frac{cyQ^2(1.011Q^2 - 2.409)}{2\tilde{T}} + c[(1-\eta)^{-1} + \frac{2yQ^2(1.011Q^2 - 1.2045)}{\tilde{T}}] \end{aligned} \quad (9)$$

and Eq. 10 was used to calculate the  $\mu_1^P$  [23, 30],

$$\mu_1^P = G_m + x_2 \frac{\partial G_m}{\partial x_1} \quad (10)$$

where  $G_m$  is the molar free energy of the polymer-gas mixture (binary mixture system) [22, 23, 29, 30].

$$\begin{aligned} \frac{G_m}{RT} = x_1 \ln x_1 + x_2 \ln x_2 + \ln(y/s) + s \frac{1-y}{y} \ln(1-y) + (s-1) \ln \frac{e}{z-1} - c[\ln(v^*(1-\eta)^3 / Q)] \\ - \frac{3}{2} c_1 x_1 \ln \frac{2\pi m_1 RT}{(N_a h)^2} - \frac{3}{2} c_2 x_2 \ln \frac{2\pi m_2 RT}{(N_a h)^2} + \frac{cyQ^2(1.011Q^2 - 2.409)}{2\tilde{T}} \\ + \frac{c}{ms} [(1-\eta)^{-1} + \frac{2yQ^2(1.011Q^2 - 1.2045)}{\tilde{T}}] \end{aligned} \quad (11)$$

### 2. Gas blend (mixture) dissolved in polymer melt (ternary mixture system)

When the gas blend (mixture) was used, both gas components (i.e., HFC 134a and HFC 152a) will dissolve into the polymer melt and the mass distribution for each of them in the polymer-gases ternary mixture would be determined by the phase equilibrium equation (i.e., Eq. 7) as well. In this study, we denoted HFC 134a, HFC 152a, and PS as components 1, 2, and 3, respectively. When the phase equilibrium was established, the chemical potential for each component (1 and 2) should be

identical in all phases (i.e., vapor or polymer-gas mixture phase). Therefore, the following coupled equations (Eq. 12 and 13) should be applied to determine the equilibrium condition. Hence the theoretical solubility will be obtained afterwards.

$$\mu_1^G(P, T) = \mu_1^P(P, T, X_{theory,1}) \quad (12)$$

$$\mu_2^G(P, T) = \mu_2^P(P, T, X_{theory,2}) \quad (13)$$

where  $\mu_1^G$  and  $\mu_2^G$  are the chemical potential of component 1 and component 2, respectively, in the gas blend (binary mixture) phase, which could be determined using Eq. 10 and 11.  $\mu_1^P$  and  $\mu_2^P$  are the chemical potential of component 1 and component 2, respectively, in the polymer-gas blend (ternary mixture) phase. They could be calculated as shown below:

$$\mu_1^P = G_m + (1 - x_1) \frac{\partial G_m}{\partial x_1} - x_2 \frac{\partial G_m}{\partial x_2} \quad (14)$$

$$\mu_2^P = G_m - x_1 \frac{\partial G_m}{\partial x_1} + (1 - x_2) \frac{\partial G_m}{\partial x_2} \quad (15)$$

where  $G_m$  is the molar free energy of the polymer-gas blend mixture (ternary mixture) [22, 29].

$$\begin{aligned} \frac{G_m}{RT} = & x_1 \ln x_1 + x_2 \ln x_2 + x_3 \ln x_3 + (s-1) \ln \frac{e}{z-1} + \ln(y/s) + s \frac{1-y}{y} \ln(1-y) \\ & - c[\ln(v^*(1-\eta)^3/Q)] + \frac{cyQ^2(1.011Q^2 - 2.409)}{2\tilde{T}} \\ & - \frac{3}{2} c_1 x_1 \ln \frac{2\pi m_1 RT}{(N_a h)^2} - \frac{3}{2} c_2 x_2 \ln \frac{2\pi m_2 RT}{(N_a h)^2} - \frac{3}{2} c_3 x_3 \ln \frac{2\pi m_3 RT}{(N_a h)^2} \\ & + c[(1-\eta)^{-1} + \frac{2yQ^2(1.011Q^2 - 1.2045)}{\tilde{T}}] \end{aligned} \quad (16)$$

Using Eq. 12 through 16 together with the SS EOS (i.e., Eq. 4 and 5), the solubility for each gas component in the polymer melt could be obtained.

## Results and Discussion

### Determination of scaling parameters for SS EOS

As usual, the SS EOS scaling parameters of all the components (HFC 134a, HFC 152a and PS) were optimized from the thermodynamic properties for each of the components. In details, the gas-liquid saturation curves that were up to the critical point were applied to extract the scaling parameters for HFC 134a and HFC 152a, respectively. The fitting results were shown in Fig. 2 and Fig. 3.

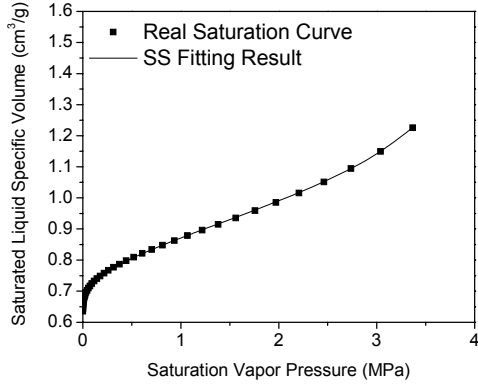


Figure 2 SS fitting result for the saturation curve of HFC 134a

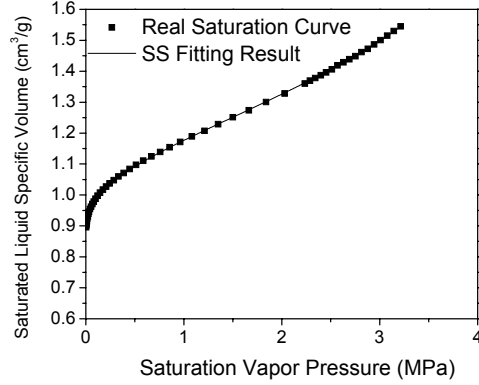


Figure 3 SS fitting result for the saturation curve of HFC 152a

For PS, the PVT data computed using Eq. 2 was used as the experimental data in order to extract the optimal scaling parameters for the SS EOS to yield the best PVT fitting, which is illustrated in Fig. 4. As required by the SS EOS theory, the polymer segment sizes should be adjusted in such a way that the molar repulsion volumes of the polymer segments match those of the gas molecules [23]. Therefore, in accordance with the polymer/gas system being studied, the SS scaling parameters for PS were obtained. All SS scaling parameters for each component are listed in Table 1.

Table 1. Scaling parameters for SS-EOS.

<i>SS Parameters</i>	<i>HFC 134a</i>	<i>HFC 152a</i>	<i>PS 685D</i>
$P^*$ (MPa)	308.7	367.5	807.8
$V^*$ (cc/g)	0.6146	0.8418	0.9621
$T^*$ (K)	5583.8	5610.3	16044
S	1	1	3204.3
C	0.4170	0.4384	500.64
M (g/mole)	102.03	66.1	$1.96 \times 10^5$

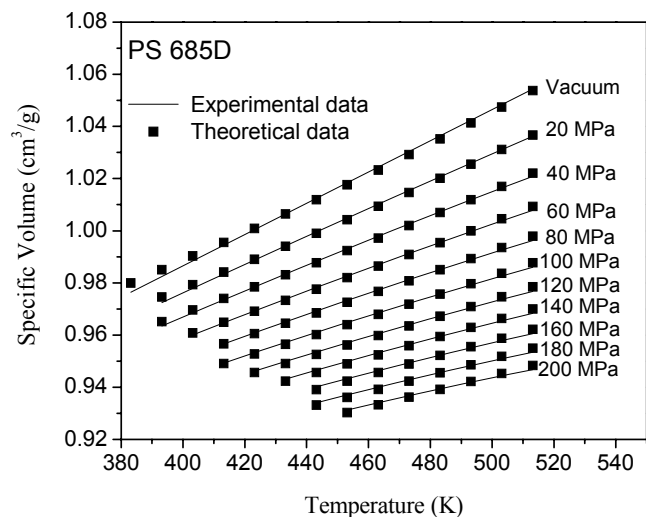


Figure 4 SS fitting result for the PVT of PS 685D

### Pure Gas Solubility Determination

As discussed in the Theoretical Framework section, the solubility of pure HFC 134a and HFC 152a in PS at 150 °C and 190 °C was successfully obtained up to 800 psi on the basis of MSB-measured apparent solubility. It is known that the overall volume of the polymer–gas mixture swelled due to the dissolution of gas in the polymer melt. In order to determine the amount of swollen volume due to the gas dissolution, SS EOS (Eq. 4 and 5) was adopted in this study. Therefore the corrected solubility was compensated with an SS-based swollen volume prediction. As shown in Fig. 5, the solubility for both HFC 134a and HFC 152a in PS increases as the pressure increases and temperature decreases. Compared with HFC 152a, the solubility of HFC 134a in PS was much lower. Our measured solubility data matches very well with other data from the literature [5, 6].

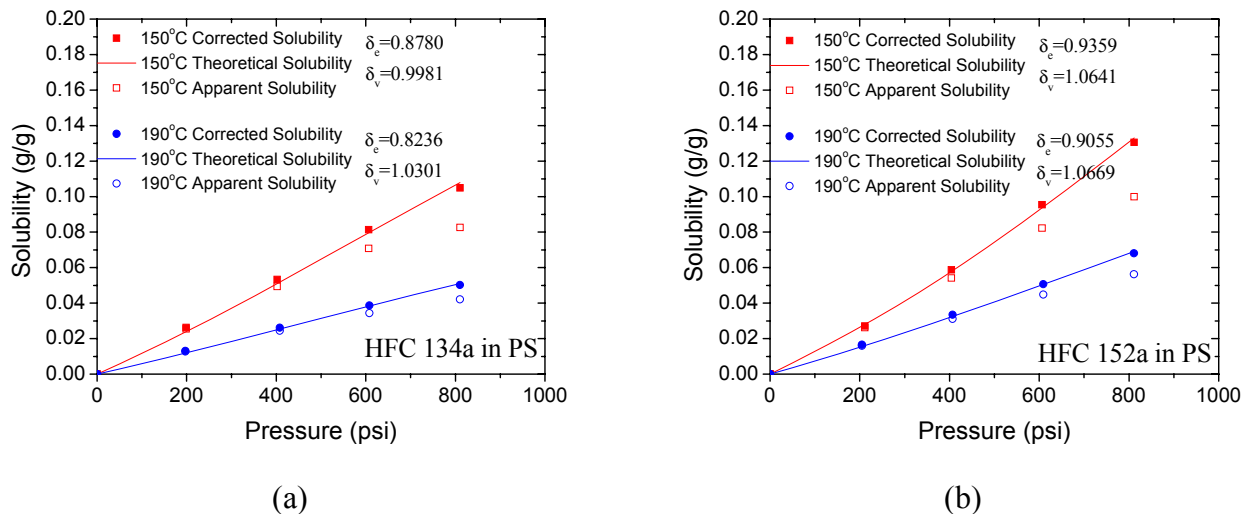


Figure 5 Solubility of (a) pure HFC 134a and (b) pure HFC 152a in PS at 150°C and 190°C

## Gas Blend Solubility Determination

In this study, the gas blend (i.e., HFC 134a and HFC 152a) with fixed composition (mass ratio between HFC 134a and HFC 152a is 50:50) was used for the sorption experiment. The overall solubility of the gas blend along with each individual component's solubility was investigated. Using the swollen volume compensation predicted by the SS EOS, the overall solubility of the gas blend was obtained. The result was shown in Fig. 6. It was observed that the overall solubility of the gas blend followed the same trend as that of the pure gas did. Moreover, it is less than that of pure HFC 152a and higher than that of HFC 134a under the same temperature and pressure. It is obvious that the solubility of the gas blend will be affected by the gas blend composition because of the different solubility of these gases.

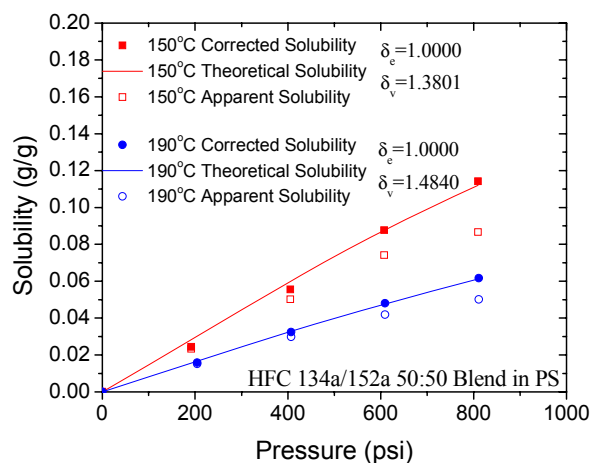


Figure 6 Overall solubility of HFC 134a and HFC 152a blend (mass ratio 50:50) in PS

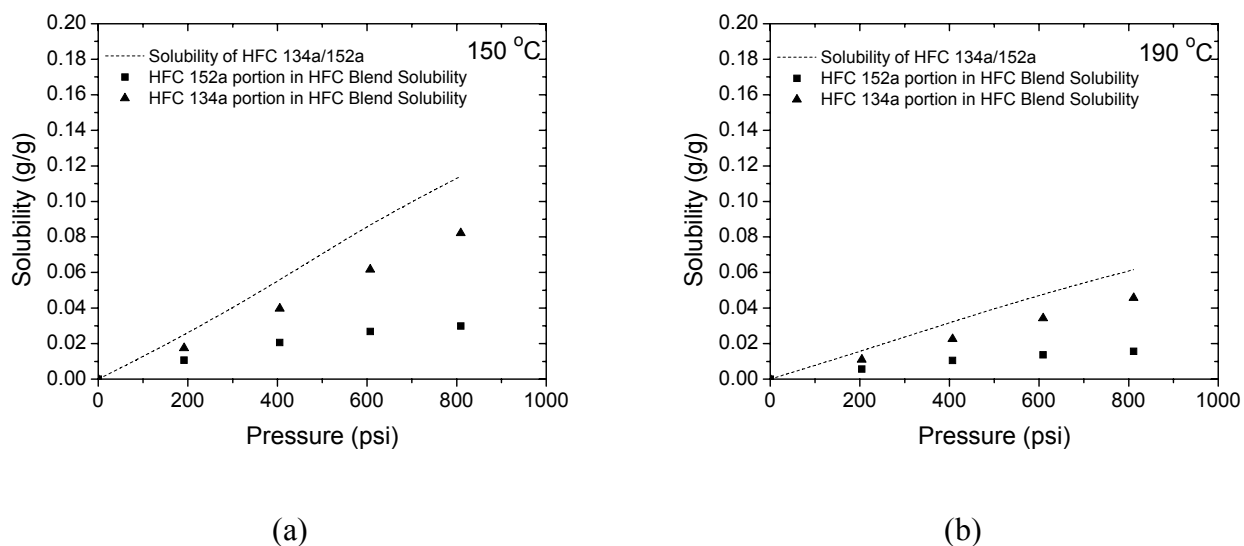


Figure.7 Solubility of (a) pure HFC 134a and (b) pure HFC 152a in PS at 150°C and 190°C

Besides the overall solubility of the gas blend, it is very important to know the solubility of each component and how the presence of one component in the gas blend affects the other component.

Based on the calculation (see Fig. 7), it is observed that even though the gas blend composition is fixed at 50:50 (mass ratio), the dissolved HFC 152a content is higher than the dissolved HFC 134a content in the polymer melt. It is assumed that the higher solubility of HFC 152a is caused by the higher partial pressure of HFC 152a in the gas blend's vapor phase when compared to that of HFC 134a.

#### Solubility Pressure for the Polymer Melt with Dissolved Gas Blend

During the plastic foam processing, it is very helpful for researchers to know the moment at which the phase separation or nucleation will occur during the pressure drop process being applied to the polymer-gas mixture. The pressure where the nucleation should occur is called solubility pressure, which is determined by the dissolved gas content and system temperature etc. When the gas blend is applied, both the solubility pressure and the compositions of the nucleated vapor phase are very helpful information. In other words, with a fixed total amount of the injected gases in the polymer, which has given composition between HFC 134a and HFC 152a, how do these two components behave during the nucleation?

Table 2-a Solubility pressure and Vapor Composition at 150 °C

Mass Ratio in the Injected BAs (HFC 134a:HFC 152a)	Solubility Pressure (MPa)	HFC 134a Composition in Vapor	HFC 152a Composition in Vapor
<b>150 °C, 6%</b>			
25:75	2.5324	0.3869	0.6131
50:50	2.7264	0.6331	0.3669
75:25	2.7354	0.8296	0.1704
<b>150 °C, 8%</b>			
25:75	3.3130	0.4230	0.5770
50:50	3.7014	0.6348	0.3652
75:25	3.6374	0.8085	0.1915
<b>150 °C, 10%</b>			
25:75	4.1395	0.4487	0.5513
50:50	4.8670	0.6367	0.3633
75:25	4.6407	0.7865	0.2135
<b>150 °C, 12%</b>			
25:75	4.8675	0.4754	0.5246
50:50	6.5558	0.6405	0.3595
75:25	5.8332	0.7555	0.2445

In this study, a given amounts of gas blend with various compositions were assumed to be injected and dissolved into the polymer melt. Consequently, the corresponding equilibrium condition (solubility pressure) was calculated using the SS EOS. Moreover, the gas composition of the vapor phase in equilibrium was also obtained. At both 150 °C and 190 °C, we have varied the total amount of injected gas blend and the composition of the injected gas blend. The corresponding solubility pressure and vapor composition were shown in Table 2. It is observed that the solubility pressure increased with the increase of the total injected gas amount. On the other hand, at a given amount of injected gas blend, the mass ratio between the HFC 134a and HFC 152a in the injected gas blend will affect the solubility

as well. Due to the fact that HFC 152a is more soluble than HFC 134a, the ratio between HFC 134a and HFC 152a in the polymer melt is much less than that in the vapor phase. These findings indicate that when the gas blend was applied in the foaming process, the less soluble component tends to diffuse out more rapidly than the more soluble component during the phase separation and nucleation.

Table 2-b Solubility pressure and Vapor Composition at 190 °C

Mass Ratio in the Injected BAs (HFC 134a:HFC 152a)	Solubility Pressure (MPa)	HFC 134a Composition in Vapor	HFC 152a Composition in Vapor
<b>190 °C, 3%</b>			
25:75	2.3829	0.4076	0.5924
50:50	2.6065	0.6670	0.3330
75:25	2.7326	0.8694	0.1306
<b>190 °C, 4%</b>			
25:75	3.1852	0.4340	0.5660
50:50	3.5708	0.6657	0.3343
75:25	3.6695	0.8502	0.1498
<b>190 °C, 5%</b>			
25:75	4.0446	0.4590	0.5410
50:50	4.6731	0.6644	0.3356
75:25	4.6955	0.8309	0.1691
<b>190 °C, 6%</b>			
25:75	4.9990	0.4831	0.5169
50:50	6.0316	0.6630	0.3370
75:25	5.8807	0.8104	0.1896

## Conclusions

This paper developed a methodology to measure the solubility of gas mixtures in a polymer melt. Due to the volume swelling of the polymer/gas mixtures, the experimentally-measured apparent solubility data was corrected by considering the buoyancy effect related to the swollen volume for the polymer/gas mixtures. As a case example, the solubility of HFC 134a and HFC 152a in the polystyrene melt was measured up to 800 psi at 150 °C and 190 °C. The apparent solubility was experimentally measured by a magnetic suspension balance. The Simha-Somcynsky (SS) equation of state (EOS) was applied in the multi-component system to estimate the swollen volume and thereby obtain the buoyancy compensation for the determination of the solubility. The overall solubility of the gas blend is less than that of HFC 152a and higher than that of HFC 134a under the same temperature and pressure. It was also found that HFC 152a component has a higher solubility than HFC 134a component in the gas blend. When the gas blend was applied in the polymeric foaming process, a larger amount of the less soluble component tends to diffuse out during the phase separation and nucleation.

## Acknowledgments

The authors are grateful to the AUTO 21 and the Consortium for Cellular and Microcellular Plastics (CCMCP) for their financial support.

## References

- [1] Park, C. B.; Behraves, A. H.; Venter, R. D. *Polym Eng Sci* 1998, 38, 1812-1823.
- [2] Suh, K. W.; Park, C. P.; Maurer, M. J.; Tusim, M. H.; De Genova, R.; Broos, R.; Sophiea, D. P. *Advanced Materials* (Weinheim, Germany) 2000, 12, 1779-1789.
- [3] Klemperer, D.; Frisch, K. C. *Handbook of Polymeric Foams and Foam Technology*; Oxford University Press: Munich; Vienna; New York, 1991.
- [4] Sato, Y.; Iketani, T.; Takishima, S.; Masuoka, H. *Annual Technical Conference - Society of Plastics Engineers* 1999, 57th, 3839-3843.
- [5] Sato, Y.; Iketani, T.; Takishima, S.; Masuoka, H. *Polym Eng Sci* 2000, 40, 1369-1375.
- [6] Wang, M.; Sato, Y.; Iketani, T.; Takishima, S.; Masuoka, H.; Watanabe, T.; Fukasawa, Y. *Fluid Phase Equilib* 2005, 232, 1-8.
- [7] Tomasko, D. L.; Han, X.; Liu, D.; Gao, W. *Current Opinion in Solid State & Materials Science* 2003, 7, 407-412.
- [8] Daigneault, L. E. In *Annual Technical Conference - Society of Plastics Engineers*, 2000; 2000.
- [9] Utracki, L. A.; Simha, R. *J Polym Sci Part B* 2001, 39, 342-362.
- [10] Gendron, R.; Vachon, C.; Champagne, M. F.; Delaviz, Y. *Cell Polym* 2004, 23, 1-23.
- [11] Gendron, R.; Champagne, M. F. *Annual Technical Conference - Society of Plastics Engineers* 2006, 64th, 2700-2704.
- [12] Gendron, R.; Huneault, M.; Tatibouet, J.; Vachon, C. *Cell Polym* 2002, 21, 315-341.
- [13] Sato, Y.; Fujiwara, K.; Takikawa, T.; Sumarno; Takishima, S.; Masuoka, H. *Fluid Phase Equilib* 1999, 162, 261-276.
- [14] Sato, Y.; Yurugi, M.; Fujiwara, K.; Takishima, S.; Masuoka, H. *Fluid Phase Equilib* 1996, 125, 129-138.
- [15] Sato, Y.; Takikawa, T.; Sorakubo, A.; Takishima, S.; Masuoka, H. *Ind Eng Chem Res* 2000, 39, 4813-4819.
- [16] Sato, Y.; Takikawa, T.; Takishima, S.; Masuoka, H. *The journal of Supercritical fluids* 2001, 19, 187-198.
- [17] Sato, Y.; Takikawa, T.; Yamane, M.; Takishima, S.; Masuoka, H. *Fluid Phase Equilib* 2002, 194-197, 847-858.
- [18] Areerat, S.; Hayata, Y.; Katsumoto, R.; Kegasawa, T.; Egami, H.; Ohshima, M. *J Appl Polym Sci* 2002, 86, 282-288.
- [19] Li, G.; Li, H.; Wang, J.; Park, C. B. *Annual Technical Conference - Society of Plastics Engineers* 2005, 63rd, 2332-2336.
- [20] Li, G.; Li, H.; Turng, L. S.; Gong, S.; Zhang, C. *Fluid Phase Equilib* 2006, 246, 158-166.
- [21] Simha, R.; Somecynsky, T. *Macromolecules* 1969, 2, 342-350.
- [22] Jain, R. K.; Simha, R. *Macromolecules* 1980, 13, 1501-1508.
- [23] Simha, R.; Moulinie, P. In *Foam Extrusion: Principles and Practice*; Lee, S.T. Eds.; Technomic: Lancaster, 2000; pp. 344.
- [24] Li, G.; Li, H.; Turng, L. S.; Gong, S. *Annual Technical Conference - Society of Plastics Engineers* 2006, 64th, 2684-2690.
- [25] Kleinrahm, R.; Wagner, W. *J.Chem.Thermodyn.* 1986, 18, 739.
- [26] Dreisbach, F.; Losch, H. W. *Journal of Thermal Analysis and Calorimetry* 2000, 62, 515-521.

- [27] Moore, W. J. Physical Chemistry; Prentice-Hall, INC.: Englewood Cliffs, New Jersey, 1972.
- [28] Prausnitz, J. M. Molecular thermodynamics of fluid-phase equilibria; Prentice-Hall: Englewood Cliffs, N.J., 1986.
- [29] Jain, R. K.; Simha, R. *Macromolecules* 1984, 17, 2663-2668.
- [30] Xie, H.; Simha, R. *Polym Int* 1997, 44, 348-355.